

# Fragility of Topology under Electronic Correlations in Iron Chalcogenides

Younsik Kim,<sup>1,\*</sup> Junseo Yoo,<sup>1</sup> Sehoon Kim,<sup>1</sup> Kiyohisa Tanaka,<sup>2</sup> Li Yu,<sup>3,4</sup> Minjae Kim,<sup>5,†</sup> and Changyoung Kim<sup>1,‡</sup>

<sup>1</sup>*Department of Physics and Astronomy, Seoul National University, Seoul, Korea*

<sup>2</sup>*National Institutes of Natural Science, Institute for Molecular Science, Okazaki, Japan*

<sup>3</sup>*Beijing National Laboratory for Condensed Matter Physics and Institute of Physics, Chinese Academy of Sciences, Beijing 100190, P. R. China*

<sup>4</sup>*University of Chinese Academy of Sciences, Beijing 100049, P. R. China*

<sup>5</sup>*Korea Institute for Advanced Study, Seoul, Korea*

(Dated: July 24, 2025)

The interplay between electronic correlations and topology is a central topic in the study of quantum materials. In this work, we investigate the impact of the orbital-selective Mott phase (OSMP) on the topological properties of  $\text{FeTe}_{1-x}\text{Se}_x$  (FTS), an iron chalcogenide superconductor known to host both non-trivial  $Z_2$  topology and strong electronic correlations. Using angle-resolved photoemission spectroscopy, we track the evolution of topological surface states across various doping levels and temperatures. We identify a topological phase transition between trivial and non-trivial topology as a function of selenium content, with critical behavior observed between  $x = 0.04$  and  $x = 0.09$ . Additionally, we find that at elevated temperatures, the coherence of the topological surface state deteriorates due to the emergence of OSMP, despite the topological invariant remaining intact. Our results demonstrate that the non-trivial topology in iron chalcogenide is fragile under strong electronic correlations.

## I. INTRODUCTION

With the discovery of topological phases in condensed matter, intriguing and unprecedented phenomena have been reported in materials with non-trivial topological invariants. A notable aspect of the non-trivial topology is that topological properties can be effectively coupled with various degrees of freedom therein, allowing extended functionalities [1, 2]. A representative example of this is topological superconductivity induced by the co-emergence of the non-trivial  $Z_2$  topology and superconductivity in  $\text{FeTe}_{1-x}\text{Se}_x$  (FTS) [3, 4]. In this context, it has been extensively studied how topological phases are coupled with other degrees of freedom.

On the other hand, emergent phases in quantum materials typically involve electronic correlation. In unconventional superconductors, for instance, electronic correlations are crucial ingredients for the emergence of superconductivity [5, 6]. However, topology has been mainly discussed within the concept of an effective single-particle scheme, where electron quasiparticles are independent fermions. This scheme is no longer an appropriate description when many-body electronic correlation effects set in [2, 7]. An extreme case is the Mott insulating phase from strong electronic correlations, in which the associated electron is spatially localized, resulting in a diverging incoherence of the electron's quasiparticle with a diminishing residue. Therefore, investigating how topological invariants evolve as a function of the quasiparticle residue can provide new insights into the interplay between topology and such correlation effects. It is note-

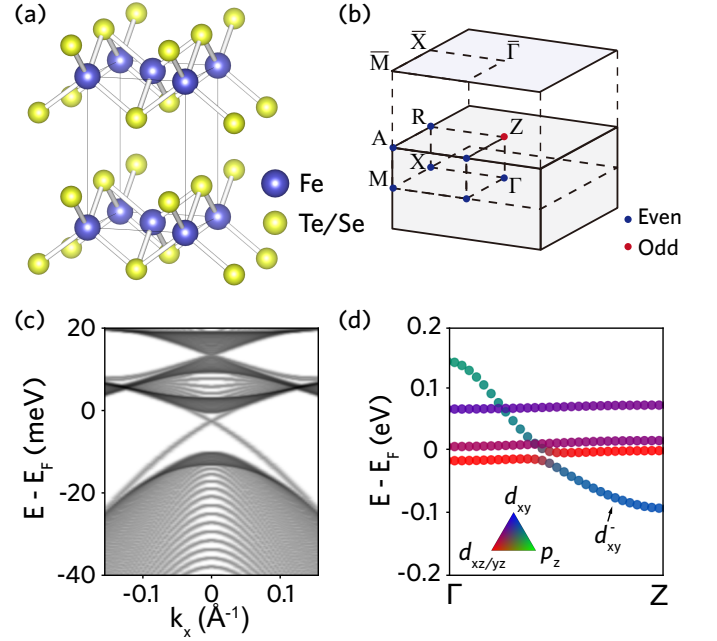


**Figure 1. Crystal and electronic structure of  $\text{FeTe}_{1-x}\text{Se}_x$  (FTS)** (a) Crystal structure of FTS. (b) Schematic of the Brillouin zone of FTS. Blue and red dots at the time-reversal invariant momentum points indicate the even and odd parities of the bands, respectively. (c) First-principles calculation of the projected band structure onto surface Brillouin zone along  $\bar{\Gamma} - \bar{X}$ . (d) First-principles calculation of the band structure along  $\Gamma - Z$ . Blue, red, and green colors correspond to the projected orbital character of  $d_{xy}$ ,  $d_{xz/yz}$ , and  $p_z$ , respectively. The weight of the  $p_z$  orbital is multiplied by a factor of 4 for better visualization.

\* leblang@snu.ac.kr

† garix.minjae.kim@gmail.com

‡ changyoung@snu.ac.kr

worthy that  $\text{SmB}_6$  is a canonical system exhibiting non-trivial topology in a strongly correlated regime [8–10].

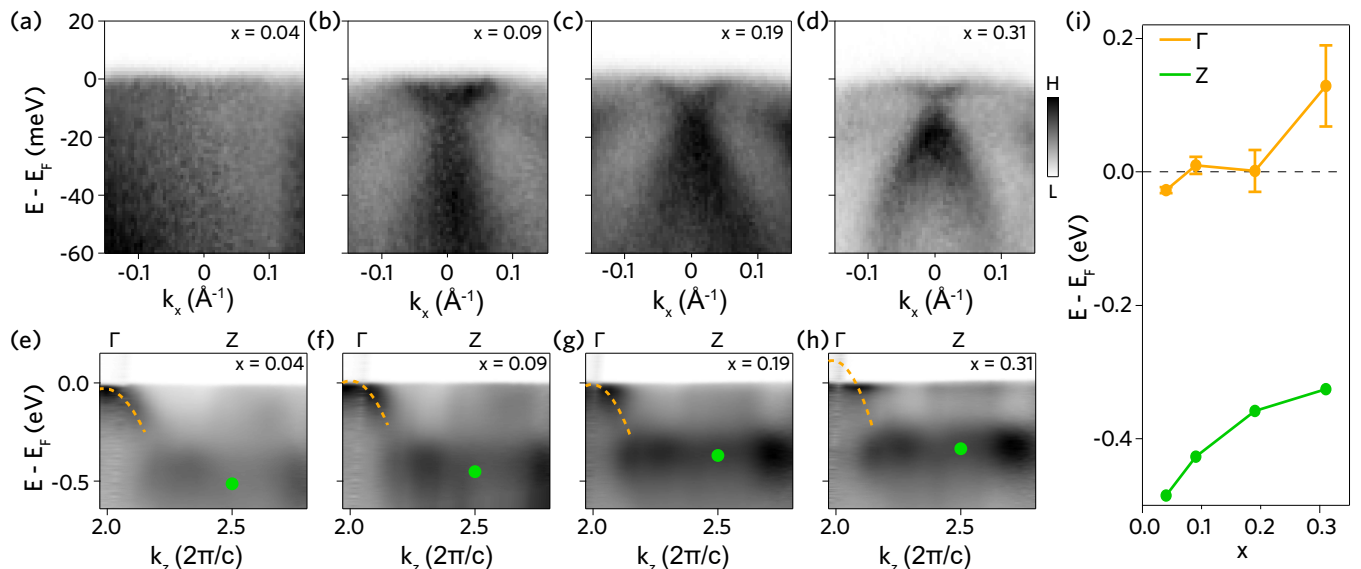


Figure 2. **Doping dependence of the electronic structures of FTS.** (a-d) Band dispersion along  $\bar{\Gamma} - \bar{X}$ , recorded with a  $p$ -polarized 7 eV light at a temperature of 15 K, with selenium contents of  $x = 0.04, 0.09, 0.19$ , and  $0.31$ , respectively. (e-h) Band dispersion along  $\Gamma - Z$  at 15 K, with selenium contents of  $x = 0.04, 0.09, 0.19$ , and  $0.31$ , respectively. The yellow dashed lines and green dots represent the fitted peak positions of the  $d_{xy}^-$  band near the  $\Gamma$  point and at the  $Z$  point, respectively. (i) Energy of the odd-parity  $d_{xy}^-$  band at the  $\Gamma$  point (yellow line) and  $Z$  point (green line) as a function of selenium content  $x$ . Error bars represent the standard deviation obtained from multiple fittings using different random seeds.

However, detailed investigation of the topological surface state has been hindered by the limited accessibility of laser-based ARPES and the surface state's sensitivity to impurity levels [11, 12].

FTS represents an ideal platform for examining this interplay, as it simultaneously hosts non-trivial  $Z_2$  topology and an orbital-selective Mott phase (OSMP) as a function of Se contents [13]. The OSMP is a unique state where one band becomes localized while others remain itinerant [14, 15]. By controlling temperature and chemical doping, the quasiparticle residue of the localized orbital can be effectively tuned in the vicinity of the OSMP, thereby modulating the topological properties. Employing angle-resolved photoemission spectroscopy (ARPES), we could directly observe and map this topological phase transition. Specifically, we observed a topological phase transition at the lightly Se-doped regime in FTS, resulting in trivial topology at the Te end. Temperature-dependent measurements reveal no significant band renormalization, which conserves the topological invariant. However, the topological surface state becomes rapidly incoherent at elevated temperatures, which is an indication of broken topological properties. Our systemic doping- and temperature-dependent study gives crucial insight into the relationship between OSMP and non-trivial topology.

## II. RESULTS

FTS has the simplest crystal structure among iron-based superconductors (Fig. 1(a)), yet it exhibits diverse phenomena as a function of chalcogen contents, as shown in the sensitively controlled correlated electronic structures [14]. Non-trivial  $Z_2$  topology is a prime example; it arises from a band inversion along the  $\Gamma - Z$  direction, leading to an odd-parity occupied band at the  $Z$  point, while bands at other time-reversal invariant momenta remain even parity (see Fig. 1(b)) [3, 16, 17]. As a result of the band inversion, a Dirac surface state is formed at the  $\Gamma$  point (Fig. 1(c)). This band inversion is associated with the crossing of the odd-parity  $d_{xy}^-$  and even-parity  $d_{xz}$  bands near the Fermi level (Fig. 1(d)). The odd-parity band is a hybridized state with  $d_{xy}^-$  and  $p_z$  orbitals [17]. We hereafter define the odd-parity band as the  $d_{xy}^-$  band. Due to the significant interlayer overlap of  $p_z$  orbitals, the odd-parity band is highly dispersive along the  $k_z$  direction as illustrated in Fig. 1(d). This significant overlap and hybridization make the position of the  $d_{xy}^-$  band sensitive to the Se/Te ratio, which allows us to control the topological properties [16, 17]. With its highly tunable topology and the presence of an OSMP, FTS provides an ideal platform to explore the interplay between electronic correlations and topology.

To reveal the topological properties of iron chalcogenide superconductors in the strongly correlated limit, we investigated the Dirac surface state using high-resolution laser-based ARPES. Figure 2a-d show the laser-based ARPES results near the  $\Gamma$  point obtained

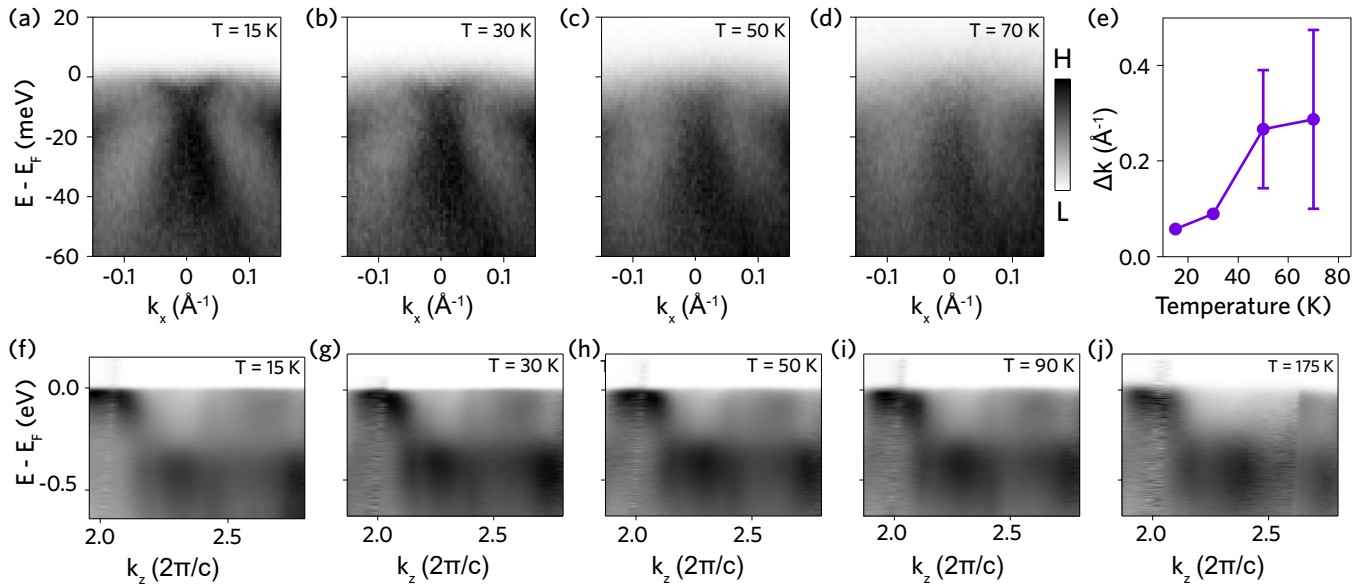


Figure 3. **Temperature dependence of the electronic structures of FTS.** (a-d) Band dispersion along  $\bar{\Gamma} - \bar{X}$ , recorded with  $p$ -polarized 7 eV light at temperatures of 15, 30, 50, 70 K, with a selenium content of  $x = 0.19$ , respectively. (e) Full width at half maximum of the Dirac surface state as (f-j) Band dispersion along  $\Gamma - Z$  with selenium contents of  $x = 0.09$  at temperatures of 15, 30, 50, 70, and 175 K, respectively.

with selenium contents  $x$  of 0.04, 0.09, 0.19, and 0.31, respectively. The ARPES results reveal that the dopings of  $x = 0.09$ , 0.19, and 0.31 show the Dirac surface state (Fig. 2(b-d)), while the doping of  $x = 0.04$  does not show the Dirac surface state (Fig. 2(a)).

To further investigate the origin of the missing Dirac cone, we performed ARPES measurements along the  $k_z$  direction on FTS with the same doping series. Shown in Fig. 2(e-h) are the electronic structures of FTS along the  $\Gamma - Z$  line with selenium contents of  $x = 0.04$ , 0.09, 0.19, and 0.31, respectively. They all show a dispersive band, which can be attributed to the  $d_{xy}^-$  band. To track the evolution of the  $d_{xy}^-$  band as a function of doping, the top and bottom positions of the band at the  $\Gamma$  and  $Z$  points, respectively, are extracted from two-dimensional fittings as shown in Fig. 2(i) (see Supplementary Information (SI) for details of the fitting) [18]. The  $d_{xy}^-$  band overall moves towards lower energy for lower Se contents. This doping-dependent evolution of the  $p_z$  band is consistent with previous calculations on  $\text{FeTe}_{0.55}\text{Se}_{0.45}$  and  $\text{FeSe}$  [16]. The notable point of the doping-dependent evolution is that the band at the top of the  $d_{xy}^-$  band at the  $\Gamma$  point goes below the Fermi level at  $x = 0.04$ . If the  $d_{xy}^-$  band goes below the  $d_{xz}$  band, which is near the Fermi level, this makes the inversion parities of the  $\Gamma$  and  $Z$  both odd, resulting in trivial topology. Taking into account the ARPES results shown in Fig. 2, we conclude that the topological phase transition occurs between  $x = 0.04$  and 0.09, resulting in a trivial topology in  $x = 0.04$ .

Another notable aspect of the evolution of the  $d_{xy}^-$  band is that the overall bandwidth does not change considerably as a function of doping. This behavior cannot be

solely explained without correlation effects, as a previous study based on the density functional theory predicted that the bandwidth of  $d_{xy}^-$  increases with Te doping since Te doping enhances the interlayer coupling from the out-of-plane tunneling of the chalcogen  $p_z$  orbital [16]. In addition to the aforementioned non-interacting term, the correlation effect renormalizes the  $d_{xy}^- - p_z$  hybridization by a factor of  $\sqrt{Z_{xy}}$  where  $Z_{xy}$  is the quasiparticle residue of  $d_{xy}$  orbital [17]. These two opposite terms compensate for each other while  $1/Z_{xy}$  (the effective mass of  $d_{xy}$ ) does not diverge at low temperatures, resulting in an unchanged bandwidth.

Having established the doping dependence of topology at the lightly Se-doped limit, we now investigate the temperature dependence of the Dirac surface state on the compound with  $x = 0.19$ , which exhibits a clear Dirac surface state at low temperatures. Fig. 3(a-d) illustrate the Dirac surface state with temperatures of 15 K, 30 K, 50 K, and 70 K, respectively. The Dirac surface state is well-defined at 15 K. The Dirac surface state in this compound becomes rapidly incoherent at relatively low temperatures, as evidenced by the loss of spectral weight and spectral broadening. The Dirac surface state is already nearly indistinguishable at 50 K.

To quantitatively investigate the temperature dependence of the Dirac surface state, we performed momentum distribution curve fitting of the Dirac surface state at the Fermi level and plotted the full width at half maximum as a function of temperature in Fig. 3(e) (see Methods for fitting details). An abrupt change in the mean free path is observed between 30 K and 50 K, as also seen from the blurred spectrum at 50 K. Above 50

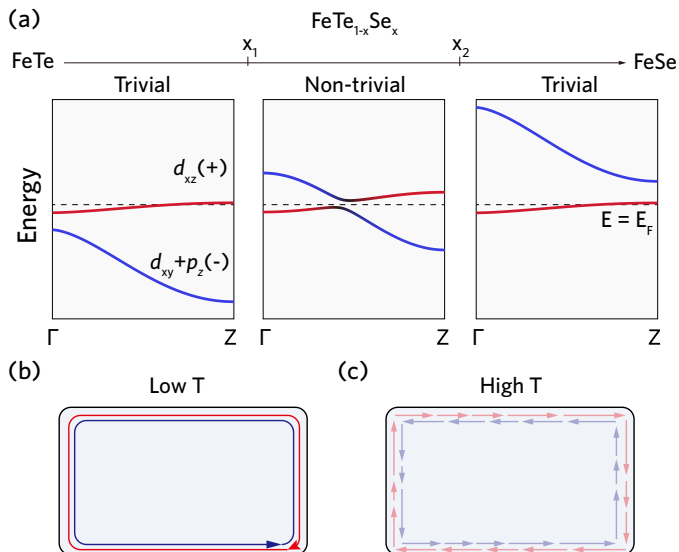


Figure 4. **Correlation and topology.** (a) Schematic of band dispersion along  $\Gamma - Z$ .  $x_1$  and  $x_2$  denote the critical selenium contents in FTS where topological phase transitions occur. (b,c) Illustration of topological surface states at low and high temperatures.

K, the mean free path estimated from the momentum width is less than 5 Å, which is strikingly short for a topologically protected surface state. Given that typical topological surface states exhibit a mean free path on the order of tens of nanometers at room temperature [19, 20], the unusually short mean free path in this compound at relatively low temperatures suggests the presence of additional modulation that scatters the topological surface state.

One possible scenario for the loss of the Dirac surface state is a transition to trivial topology at high temperatures. A previous study based on dynamic mean-field theory calculations predicted that OSMP could alter the overall band structures suppressing the band inversion, as the  $d_{xy}^-$  band disappears near the Fermi level in the OSMP [17]. To confirm this scenario, we performed ARPES measurements along the  $\Gamma - Z$  direction on the  $x = 0.09$  sample at various temperatures (Fig. 3(f-j)). The temperature-dependent ARPES spectra show that the positions of the  $d_{xy}^-$  band remain unchanged over temperature. These results suggest that the band inversion is intact up to 175 K, preserving the topological invariant. We note that 175 K is well above the OSMP temperature at  $x = 0.19$  [21].

Given that lightly Se-doped FTS exhibits an orbital-selective Mott phase (OSMP) at high temperatures, we attribute the modulation that scatters the topological surface state to the emergence of the OSMP. In FTS, the OSMP is characterized by the loss of coherence in the  $d_{xy}$  orbital at high temperatures. Since the odd parity band responsible for the non-trivial topology mainly consists of  $d_{xy}$  orbital, the onset of the OSMP significantly im-

pacts the topological surface, diminishing its coherence and spectral weight in a manner analogous to its effect on the bulk bands. These aspects will be discussed in more detail in the Discussion section.

Our results demonstrate doping- and temperature-dependent trends in the topological properties of band structures, as summarized in Fig. 4. Selenium doping sensitively controls the position of the odd-parity band, directly affecting the system's topology. Non-trivial topology emerges within a specific doping window determined by the crossing of even and odd-parity bands: while previous studies set the critical doping  $x_2$  at approximately  $x = 0.45$  [22], our findings newly establish a lower boundary  $x_1$  between  $x = 0.04$  and  $x = 0.09$  (Fig. 4(a)). Additional temperature-dependent ARPES measurements reveal that the topological invariant itself remains unchanged across the studied temperature range. However, the topological surface states become significantly broadened and weakened with increasing temperature (Fig. 4(b)), resulting in a loss of their practically useful topological properties at high temperatures.

### III. DISCUSSION

Our experimental observations provide important insights into the OSMP. In a lightly Se-doped regime ( $x < 0.1$ ), the even-parity  $d_{xy}^+$  band giving a in-plane hole band dispersion has a significant mass renormalization factor  $m^*/m_{DFT}$  of more than 40, resulting in an almost complete loss of spectral weight in ARPES [15, 21, 23]. On the other hand, the odd-parity  $d_{xy}^-$  band is unexpectedly robust in this regime, even at elevated temperatures. The robust  $d_{xy}^-$  band suggests that the effective mass of the  $d_{xy}$  orbital is not diverging in the lightly Se-doped regime, which implies that the  $d_{xy}$  orbital has a small but finite quasiparticle residue ( $Z_{xy}$ ) in the observed temperature range. This scenario is further supported by the fact that the mass renormalization of  $d_{xy}^+$  is more sensitive to  $Z_{xy}$  than that of  $d_{xy}^-$ , given that the  $d_{xy}^+$  is a non-bonding and the  $d_{xy}^-$  is an anti-bonding from the hybridization between  $d_{xy}$  and  $p_z$  orbitals along  $\Gamma - Z$  [17]. Even without the mass divergence of  $d_{xy}$  (or zero quasiparticle residue), strong scattering induced by the spin fluctuation of  $d_{xy}$  imposes significant decoherence, making low-energy features of  $d_{xy}$  indiscernible in ARPES [21, 24–26]. It is noteworthy that such a decoherence effect is also observed in some magnetic materials, which is a manifestation of strong correlations [27, 28]. As topology is only well-defined in a single-particle scheme, the strong decoherence imposed by OSMP significantly deteriorates topological properties [2, 7].

The robust  $d_{xy}^-$  also raises a question about the existence of truly zero quasiparticle residue (mass divergence) from the OSMP, in the presence of the inter-orbital hybridizations [29]. As even FeTe shows robust  $d_{xy}^-$  [23], the experimental realization of further local-

ization of  $d_{xy}$  beyond FeTe can give more clues on this question. Possible approaches are applying hydrostatic pressure [30] or epitaxial strain on FeTe for further localization of  $d_{xy}$  [31, 32].

Recently, we became aware of a similar report that also addressed the topology of FTS in the lightly Se-doped limit. In addition to Ref. [33], our discovery of the evolution of  $d_{xy}^-$  along the  $\Gamma - Z$  direction as a function of doping and temperature gives a deeper understanding of the underlying mechanism of OSMF and its relation to the topological phase transition.

### ACKNOWLEDGEMENTS

We acknowledge S. Huh, Z. X. Shen, D.-H. Lee, and G. Kotliar for useful discussions. This work was supported by the National Research Foundation of Korea (NRF) grant funded by the Korean government (MSIT) (No.

2022R1A3B1077234) and Global Research Development Center Cooperative Hub Program (GRDC) through NRF (RS-2023-00258359). MK was supported by the KIAS Individual Grant (CG083502).

### AUTHOR CONTRIBUTIONS

Y.K., M.K., and C.K. conceived the project. Y.K. and J.Y. synthesized and characterized FTS crystals. Y.K. developed the laser ARPES system with support from L.Y. Y.K. and S.K. conducted the laser ARPES experiments. Y.K., J.Y., and S.K. carried out the synchrotron ARPES experiments with support from K.T. Y.K. analyzed the ARPES data. M.K. performed the first-principles calculations and theoretical analyses. The manuscript was written by Y.K., M.K., and C.K., with input and discussions from all authors.

- 
- [1] X.-L. Qi and S.-C. Zhang, Topological insulators and superconductors, *Reviews of modern physics* **83**, 1057 (2011).
- [2] M. Z. Hasan and C. L. Kane, Colloquium: topological insulators, *Reviews of modern physics* **82**, 3045 (2010).
- [3] P. Zhang, K. Yaji, T. Hashimoto, Y. Ota, T. Kondo, K. Okazaki, Z. Wang, J. Wen, G. D. Gu, H. Ding, *et al.*, Observation of topological superconductivity on the surface of an iron-based superconductor, *Science* **360**, 182 (2018).
- [4] P. Zhang, Z. Wang, X. Wu, K. Yaji, Y. Ishida, Y. Kohama, G. Dai, Y. Sun, C. Bareille, K. Kuroda, *et al.*, Multiple topological states in iron-based superconductors, *Nature Physics* **15**, 41 (2019).
- [5] J. Paglione and R. L. Greene, High-temperature superconductivity in iron-based materials, *Nature physics* **6**, 645 (2010).
- [6] R. Fernandes, A. Chubukov, and J. Schmalian, What drives nematic order in iron-based superconductors?, *Nature physics* **10**, 97 (2014).
- [7] S. Rachel, Interacting topological insulators: a review, *Reports on Progress in Physics* **81**, 116501 (2018).
- [8] L. Li, K. Sun, C. Kurdak, and J. Allen, Emergent mystery in the kondo insulator samarium hexaboride, *Nature Reviews Physics* **2**, 463 (2020).
- [9] M. Neupane, N. Alidoust, S. Xu, T. Kondo, Y. Ishida, D.-J. Kim, C. Liu, I. Belopolski, Y. Jo, T.-R. Chang, *et al.*, Surface electronic structure of the topological kondo-insulator candidate correlated electron system  $\text{SmB}_6$ , *Nature communications* **4**, 2991 (2013).
- [10] J. Jiang, S. Li, T. Zhang, Z. Sun, F. Chen, Z. Ye, M. Xu, Q. Ge, S. Tan, X. Niu, *et al.*, Observation of possible topological in-gap surface states in the kondo insulator  $\text{SmB}_6$  by photoemission, *Nature communications* **4**, 3010 (2013).
- [11] L. Jiao, S. Rößler, D. Kasinathan, P. F. Rosa, C. Guo, H. Yuan, C.-X. Liu, Z. Fisk, F. Steglich, and S. Wirth, Magnetic and defect probes of the  $\text{SmB}_6$  surface state, *Science Advances* **4**, eaau4886 (2018).
- [12] P. Hlawenka, K. Siemensemeyer, E. Weschke, A. Varykhalov, J. Sánchez-Barriga, N. Y. Shitsevalova, A. Dukhnenko, V. Filipov, S. Gabáni, K. Flachbart, *et al.*, Samarium hexaboride is a trivial surface conductor, *Nature Communications* **9**, 517 (2018).
- [13] J. G. Checkelsky, B. A. Bernevig, P. Coleman, Q. Si, and S. Paschen, Flat bands, strange metals and the kondo effect, *Nature Reviews Materials* **9**, 509 (2024).
- [14] M. Yi, Y. Zhang, Z.-X. Shen, and D. Lu, Role of the orbital degree of freedom in iron-based superconductors, *npj Quantum Materials* **2**, 57 (2017).
- [15] Z. Yin, K. Haule, and G. Kotliar, Kinetic frustration and the nature of the magnetic and paramagnetic states in iron pnictides and iron chalcogenides, *Nature materials* **10**, 932 (2011).
- [16] Z. Wang, P. Zhang, G. Xu, L. Zeng, H. Miao, X. Xu, T. Qian, H. Weng, P. Richard, A. V. Fedorov, *et al.*, Topological nature of the fese 0.5 te 0.5 superconductor, *Physical Review B* **92**, 115119 (2015).
- [17] M. Kim, S. Choi, W. H. Brito, and G. Kotliar, Orbital-selective mott transition effects and nontrivial topology of iron chalcogenide, *Physical review letters* **132**, 136504 (2024).
- [18] R. Kurlito and J. Fink, About two-dimensional fits for the analysis of the scattering rates and renormalization functions from angle-resolved photoelectron spectroscopy data, *Journal of Electron Spectroscopy and Related Phenomena* **253**, 147127 (2021).
- [19] M. Tian, W. Ning, Z. Qu, H. Du, J. Wang, and Y. Zhang, Dual evidence of surface dirac states in thin cylindrical topological insulator  $\text{Bi}_2\text{Te}_3$  nanowires, *Scientific reports* **3**, 1212 (2013).
- [20] Z.-H. Pan, E. Vescovo, A. Fedorov, G. Gu, and T. Valla, Persistent coherence and spin polarization of topological surface states on topological insulators, *Physical Review B—Condensed Matter and Materials Physics* **88**, 041101 (2013).
- [21] J. Huang, R. Yu, Z. Xu, J.-X. Zhu, J. S. Oh, Q. Jiang, M. Wang, H. Wu, T. Chen, J. D. Denlinger, *et al.*,

- Correlation-driven electronic reconstruction in  $\text{fete1-xse x}$ , *Communications Physics* **5**, 29 (2022).
- [22] Y. Li, N. Zaki, V. O. Garlea, A. T. Savici, D. Fobes, Z. Xu, F. Camino, C. Petrovic, G. Gu, P. D. Johnson, *et al.*, Electronic properties of the bulk and surface states of  $\text{fe1+y te1-x se x}$ , *Nature Materials* **20**, 1221 (2021).
- [23] Y. Kim, M.-S. Kim, D. Kim, M. Kim, M. Kim, C.-M. Cheng, J. Choi, S. Jung, D. Lu, J. H. Kim, *et al.*, Kondo interaction in  $\text{fete}$  and its potential role in the magnetic order, *Nature communications* **14**, 4145 (2023).
- [24] P.-H. Lin, Y. Texier, A. Taleb-Ibrahimi, P. Le Fèvre, F. Bertran, E. Giannini, M. Grioni, and V. Brouet, Nature of the bad metallic behavior of  $\text{fe 1.06 te}$  inferred from its evolution in the magnetic state, *Physical review letters* **111**, 217002 (2013).
- [25] E. Ieki, K. Nakayama, Y. Miyata, T. Sato, H. Miao, N. Xu, X.-P. Wang, P. Zhang, T. Qian, P. Richard, *et al.*, Evolution from incoherent to coherent electronic states and its implications for superconductivity in  $\text{fete 1-x se x}$ , *Physical Review B* **89**, 140506 (2014).
- [26] Z. Liu, M. Yi, Y. Zhang, J. Hu, R. Yu, J.-X. Zhu, R.-H. He, Y. Chen, M. Hashimoto, R. Moore, *et al.*, Experimental observation of incoherent-coherent crossover and orbital-dependent band renormalization in iron chalcogenide superconductors, *Physical Review B* **92**, 235138 (2015).
- [27] S. Hahn, B. Sohn, M. Kim, J. R. Kim, S. Huh, Y. Kim, W. Kyung, M. Kim, D. Kim, Y. Kim, *et al.*, Observation of spin-dependent dual ferromagnetism in perovskite ruthenates, *Physical Review Letters* **127**, 256401 (2021).
- [28] S. Lee, S. Lee, S. Jung, J. Jung, D. Kim, Y. Lee, B. Seok, J. Kim, B. G. Park, L. Šmejkal, *et al.*, Broken kramers degeneracy in altermagnetic  $\text{mnte}$ , *Physical review letters* **132**, 036702 (2024).
- [29] F. B. Kugler and G. Kotliar, Is the orbital-selective mott phase stable against interorbital hopping?, *Physical review letters* **129**, 096403 (2022).
- [30] M. Bendele, A. Maisuradze, B. Roessli, S. Gvasaliya, E. Pomjakushina, S. Weyeneth, K. Conder, H. Keller, and R. Khasanov, Pressure-induced ferromagnetism in antiferromagnetic  $\text{fe 1.03 te}$ , *Physical Review B—Condensed Matter and Materials Physics* **87**, 060409 (2013).
- [31] H. Song, Y. Kim, S. Lee, S. Lee, Y. Kim, Y. Lee, and C. Kim, Growth and characterization of  $\text{fete}$  thin films under tensile strain, *Progress in Superconductivity and Cryogenics* **26**, 20 (2024).
- [32] Y. Han, W. Li, L. Cao, X. Wang, B. Xu, B. Zhao, Y. Guo, and J. Yang, Superconductivity in iron telluride thin films under tensile stress, *Physical review letters* **104**, 017003 (2010).
- [33] H. Lin, C. L. Jacobs, C. Yan, G. M. Nolan, G. Berruto, P. Singleton, K. D. Nguyen, Y. Bai, Q. Gao, X. Wu, C.-X. Liu, G. Yan, S. Choi, C. Liu, N. P. Guisinger, P. Y. Huang, S. Mandal, and S. Yang, A topological superconductor tuned by electronic correlations, arXiv preprint arXiv:2503.22888 (2025), submitted on 28 Mar 2025.